



# Upregulation of *FOXO1* contributes to lipopolysaccharide-induced pulmonary endothelial injury by induction of autophagy

Ying Zhao<sup>1#</sup>, Hui Zhang<sup>2#</sup>, Shu-Li Zhang<sup>1</sup>, Juan Wei<sup>1</sup>, Liang-Liang Zheng<sup>1</sup>, Jian-Kui Du<sup>3</sup>, Xiao-Yan Zhu<sup>3</sup>, Lai Jiang<sup>2</sup>, Yu-Jian Liu<sup>1</sup>

<sup>1</sup>School of Kinesiology, Shanghai Frontiers Science Research Base of Exercise and Metabolic Health, The Key Laboratory of Exercise and Health Sciences of Ministry of Education, Shanghai University of Sport, Shanghai, China; <sup>2</sup>Department of Anesthesiology and Surgical Intensive Care Unit, Xinhua Hospital, Shanghai Jiao Tong University School of Medicine, Shanghai, China; <sup>3</sup>Department of Physiology, Navy Medical University, Shanghai, China

**Contributions:** (I) Conception and design: YJ Liu, XY Zhu, L Jiang; (II) Administrative support: YJ Liu, XY Zhu, L Jiang; (III) Provision of study materials or patients: Y Zhao, H Zhang, SL Zhang, J Wei, LL Zheng, JK Du; (IV) Collection and assembly of data: H Zhang, Y Zhao, SL Zhang, J Wei, LL Zheng, JK Du; (V) Data analysis and interpretation: Y Zhao, H Zhang, SL Zhang, J Wei, LL Zheng, JK Du; (VI) Manuscript writing: All authors; (VII) Final approval of manuscript: All authors.

<sup>#</sup>These authors contributed equally to this work and should be considered as co-first authors.

**Correspondence to:** Prof. Yu-Jian Liu, School of Kinesiology, The Key Laboratory of Exercise and Health Sciences of Ministry of Education, Shanghai University of Sport, 200 Hengren Road, Shanghai 200438, China. Email: liuyujian@sus.edu.cn; Prof. Lai Jiang, Department of Anesthesiology and Surgical Intensive Care Unit, Xinhua Hospital, Shanghai Jiao Tong University School of Medicine, 1665 Kongjiang Road, Shanghai 200092, China. Email: jianglai@xinhuaamed.com.cn.

**Background:** Autophagy is activated during the pathogenesis of endothelial dysfunction and sepsis-associated acute lung injury (ALI). This study aimed to investigate whether autophagy affected endothelial barrier dysfunction and lung injury in a murine model of lipopolysaccharide (LPS)-induced ALI, and then further clarify whether forkhead box O1 (*FOXO1*), an autophagy-related transcriptional factor, contributed to autophagy activation and ALI induced by LPS.

**Methods:** Male C57BL/6 mice were treated with LPS (30 mg/kg), and then were allocated to a control group and an LPS group with or without *FOXO1* inhibitor (AS1842856) treatment, respectively. Primary cultured mouse lung vascular endothelial cells (MLVECs) were treated with LPS, autophagy inhibitor 3-methyladenine (3-MA), AS1842856, and small interfering RNA (siRNA) targeting autophagy-related gene 5 (*ATG5*) or *FOXO1*. Endothelial autophagic flux was assessed by transfection of MLVECs with red fluorescent protein (RFP)-green fluorescent protein (GFP) tandem fluorescent-tagged LC3 (RFP-GFP-LC3) adenovirus. Endothelial permeability was analyzed by the diffusion of fluorescein isothiocyanate-carboxymethyl (FITC)-dextran through the endothelial monolayer. Evans blue albumin tracer was used to measure the pulmonary transvascular permeability, and hematoxylin and eosin (H&E) staining was used to observe pathological changes in the lung tissues. Immunofluorescence staining was also used to detect the expression of zonula occludens-1 (ZO-1) and *FOXO1*.

**Results:** This study found autophagy induction in lung tissues of endotoxemic mice and LPS-treated MLVECs, as evidenced by elevated expression of light chain 3 II (LC3-II) and Unc-51-like kinase (ULK1) and autophagic flux. LPS treatment decreased vascular endothelial (VE)-cadherin and ZO-1 expression and increased endothelial permeability in MLVECs, which were significantly alleviated by autophagy inhibitor 3-MA and *ATG5* siRNA. It was found that both phosphorylated *FOXO1* and *FOXO1* were upregulated in the lung tissues of endotoxemic mice and LPS-treated MLVECs. Both *FOXO1* inhibitor AS1842856 and *FOXO1* siRNA suppressed LPS-induced autophagy and endothelial cell injury in MLVECs. Moreover, *FOXO1* inhibition profoundly alleviated autophagy, lung endothelial hyperpermeability, and ALI in endotoxemic mice.

**Conclusions:** This work demonstrated that *FOXO1* upregulation is an important contributor to LPS-

induced autophagy in pulmonary VE cells. The detrimental effects of FOXO1 in endotoxemia-associated endothelial dysfunction and ALI are partly due to its potent pro-autophagic property. Inhibition of FOXO1 may be a potential therapeutic option for the treatment of ALI.

**Keywords:** lipopolysaccharide (LPS); acute lung injury (ALI); autophagy; endothelial dysfunction; forkhead box O1 (FOXO1)

Submitted Oct 09, 2021. Accepted for publication Apr 14, 2022.

doi: 10.21037/atm-21-5380

View this article at: <https://dx.doi.org/10.21037/atm-21-5380>

## Introduction

Sepsis, a systemic inflammatory condition triggered by severe infection, toxins, or trauma, is one of the foremost contributors to hospital death and represents a major global health burden (1,2). Sepsis causes multiorgan dysfunction, including acute lung injury (ALI) and acute respiratory distress syndrome (ARDS) (3). The mortality rate of patients with both sepsis and ALI/ARDS is especially high (4). Endothelial injury and consequent endothelial hyperpermeability resulting in leukocytic infiltration and influx of protein-rich fluid into the alveoli are known to be initial events in the pathogenesis of sepsis-induced ALI (5-8). Thus, elucidation of the molecular mechanisms involved in sepsis-induced pulmonary endothelial barrier dysfunction may provide new strategies for the prevention of sepsis-induced ALI/ARDS.

As an evolutionarily conserved cellular process, autophagy is known to facilitate the recycling of intracellular organelles and proteins, and play a crucial role in cell survival and body metabolism (9). Although autophagy is known to be activated during the pathogenesis of ALI, it has remained controversial whether autophagy activation alleviates or deteriorates ALI of different etiologies. For example, inhibition of autophagy protects against pulmonary endothelial cell barrier dysfunction and tissue injuries in rodent ALI models induced by lipopolysaccharide (LPS) (10), sepsis (11), and H9N2 influenza virus (12). In contrast, Zhao *et al.* reported that autophagy activation improves lung injury and inflammation in sepsis (13). Therefore, further studies are needed to investigate the role of autophagy in pulmonary endothelial hyperpermeability and its relevance in the context of ALI.

Forkhead box protein O1 (FOXO1), which belongs to the FOXO family of transcription factors, has been shown to be involved in cellular proliferation, apoptosis, autophagy, oxidative stress, and metabolic dysregulation (14). It has

been recognized as an essential regulator of vascular growth that couples metabolic and proliferative activities in endothelial cells which are highly sensitive to changes in FOXO1 activity (15). Notably, a recent study indicated that inhibition of FOXO1 protects against LPS-induced endothelial barrier injury (16).

In this study, we first investigated whether and how autophagy affected endothelial barrier dysfunction and lung injury in a murine LPS-induced ALI model, and then further clarified whether FOXO1 contributed to autophagy activation, endothelial barrier dysfunction, and ALI induced by LPS. We present the following article in accordance with the ARRIVE reporting checklist (available at <https://atm.amegroups.com/article/view/10.21037/atm-21-5380/rc>).

## Methods

### *Mouse endotoxemia model and AS1842856 treatment*

A total of 56 male C57BL/6 mice (6–8 weeks) were purchased from Shanghai Nanfang Model Organism (Shanghai, China). Animals were housed in standard cages with food and water ad libitum. Experiments were performed under a project license (No. 2016014) granted by the Animal Ethics Committee of Shanghai Sports University and in accordance with the National Institutes of Health guidelines for the care and use of animals. Male mice were randomly allocated by weight to the following four groups: control group (n=14), LPS group (n=14), AS1842856 group (n=14), LPS with AS1842856 group (n=14). Purified LPS extracted from the membrane of *Escherichia coli* 0111:B4 (Sigma-Aldrich, Saint Louis, USA) was dissolved in sterile pyrogen-free saline and injected intraperitoneally (i.p.) at a dose of 30 mg/kg, mice conforming to sepsis model were used for subsequent experiments (17). FOXO1 inhibitor AS1842856 (Selleck, Shanghai, China) was injected intragastrically (i.g.) 30 minutes before the injection of LPS at a dose of 30 mg/kg.

The chosen dose of AS1842856 was based on previous study (9) and our preliminary experiments. A protocol was prepared before the study without registration.

#### *Mouse lung vascular endothelial cells (MLVECs) isolation and culture*

MLVECs were isolated from A total of 48 male Institute of Cancer Research (ICR) mice (3–4 weeks,) as previously described (18,19). Briefly, after anesthesia, the right ventricle of mice was injected with PBS to clear blood from lungs. Peripheral, subpleural lung tissues were cut into pieces and cultured in DMEM containing 20% fetal calf serum, 25 mM HEPES, 3.7 g/L NaHCO<sub>3</sub>, 5 mg/mL heparin, 1 mg/mL hydrocortisone, 80 mg/mL endothelial cell growth supplement from bovine brain, 5 mg/mL amphotericin and 0.01% ampicillin/streptomycin at 37 °C with 5% CO<sub>2</sub> for 60 hours. Subsequently, the diced tissue was removed and the adherent cells were cultured in basal culture medium. The MLVECs passaged between 3 and 4 times were used in experiments.

#### *Transfection of small interfering RNA (siRNA)*

The siRNAs for autophagy-related gene 5 (*ATG5*) and *FOXO1* were synthesized by GenePharma Corporation (Shanghai, China). Two siRNA sequences for *ATG5* were: 5'-GCUUCGAGAUGUGUGGUUUTT-3' and 5'-AAACCACACAUCUCGAAGCTT-3'; 5'-CCAUCAACCGGAAACUCAUTT-3' and 5'-AUGAGUUUCCGGUUGAUGGTT-3' (20); Two siRNA sequences for *FOXO1* were: 5'-UGUAAUGAUGGGCCC UAAUTT-3' and 5'-AUUAGGGCCCAUCAUUACATT-3'; 5'-GCGGGCUGGAAGAAUUCAATT-3' and 5'-UUGAAUUCUCCAGCCCGCTT-3' (21,22). Negative control siRNA was scrambled sequence without any specific target: 5'-UUCUCCGAACGUGUCACGUTT-3' and 5'-ACGUGACACGUUCGGAGAATT-3'. Transfection of siRNA in MLVECs was performed by using the Lipofectamine TM3000 (Thermo Fisher) according to the manufacturer's instructions.

#### *Autophagic flux*

Adenovirus expressing red fluorescent protein (RFP)-green fluorescent protein (GFP) tandem fluorescent-tagged LC3 (RFP-GFP-LC3) was constructed by Genechem

(Shanghai, China). For assessment of autophagic flux in MLVECs, cells were cultured on coverslips for 24 hours and infected with RFP-GFP-LC3 adenovirus according to the manufacturer's protocol. This dual fluorescent reporter virus is designed to monitor autophagosomes as yellow (GFP + RFP) puncta and autolysosomes as free red (RFP) puncta *in vitro* by transfection. Cells were then cultured under the indicated experimental conditions and fixed with 4% paraformaldehyde (PFA). Images were obtained with a laser confocal microscope Zeiss LSM 710 (Zeiss, Oberkochen, Germany). The number of autophagosomes and autolysosomes were counted per transfected cells in each treatment group and quantified (23).

#### *Immunofluorescence staining*

MLVECs were fixed with 4% PFA for 15 min at room temperature and incubated with PBS containing 10% goat serum, 0.3 M glycine, 1% bovine serum albumin (BSA), and 0.1% tween for 1 hour at room temperature to permeabilize the cells and block non-specific protein-protein interactions. Cells were then incubated with primary antibodies against ZO-1 (Proteintech Cat# 21773-1-AP, RRID: AB\_10733242; Rosemont, USA), FOXO1 (Cell Signaling Technology Cat# 2880, RRID: AB\_2106495; Danvers, USA) at a dilution of 1:100 overnight at 4 °C, respectively. After washes, cells were incubated with secondary antibody (Alexa Fluor<sup>®</sup> 488, Abcam, ab150081; Carlsbad, USA) at a dilution of 1:200 at 37 °C for 1 hour in the dark. Finally, nuclei were counterstained with 4',6-diamidino-2-phenylindole (DAPI) (Sigma-Aldrich). Images were observed and photos were taken under a laser confocal microscope Zeiss LSM 710 (Zeiss). Immunofluorescence signals were quantified using Image J software, and the integrated densities of immunofluorescence positive signals were measured.

#### *Fluorescein isothiocyanate-carboxymethyl (FITC)-dextran flux*

Endothelial permeability was analyzed *in vitro* by the diffusion of FITC-dextran (10-kDa, Sigma-Aldrich), through the endothelial monolayer as previously described (18). MLVECs were grown to confluence in the Transwell inserts (0.4 μM, 12-mm diameter, Corning, NY, USA). After treatment of cells, medium containing FITC-dextran with a final concentration of 1 mg/mL was then added in the top chamber of the Transwell. After 1 hour, endothelial permeability was measured by measuring the

amount of FITC-dextran in the lower compartment using a Synergy fluorescence plate reader (Bio-Tek, Cytation3, USA; excitation 485±20 nm, emission 528±20 nm).

#### ***Evans blue-albumin (EBA) tracer measurement of pulmonary transvascular permeability***

The pulmonary transvascular albumin permeability was performed as previously described (5). Briefly, EBA (40 mg/mL BSA with 1% Evans blue dye, Sigma-Aldrich) was injected into the right jugular vein of the mice and allowed to circulate in the blood vessels for 45 min. Then intravascular Evans blue was washed by PBS perfusion from the right ventricle for 2 min. Mouse lungs were excised, homogenized in 1 mL PBS, and extracted in 2 mL formamide (Sigma-Aldrich) overnight at 60 °C. Evans blue content was determined by OD620 using spectrophotometer (Bio-Tek) of the formamide extract and normalized by body weight.

#### ***Histopathological evaluation of the lung tissue***

After hematoxylin and eosin (H&E) staining, pathological changes of lung tissues were observed under a light microscope. The lung injury score was assessed by two pathologists with expertise in lung pathology. The criteria for scoring lung injury were set up as previously described (24,25): 0 = normal tissue; 1 = tiny inflammatory change; 2 = mild to moderate inflammatory changes without marked damage in the lung architecture; 3 = moderate inflammatory injury with thickening of the alveolar septa; 4 = moderate to severe inflammatory injury with the formation of nodules or areas of pneumonitis; and 5 = severe inflammatory injury with total obliteration of the field. The mean score was reported per section.

#### ***Western blotting***

Proteins were extracted from lung tissues and MLVECs using RIPA (Beyotime, Shanghai, China) containing protease and phosphatase inhibitor cocktail (Beyotime) according to the manufacturer's instructions. Protein concentrations were determined by BCA protein assay kit (Beyotime). Equal amounts of proteins (40 µg) were separated with 10% SDS-PAGE, transferred to PVDF membrane (Millipore, Billerica, MA, USA), and then blocked with 5% non-fat milk. Membranes were incubated overnight with specific primary antibodies against FOXO1

(Cell Signaling Technology Cat# 2880, RRID:AB\_2106495), Phospho-FoxO1 (Ser256) (Cell Signaling Technology Cat# 9461, RRID:AB\_329831), ATG5 (Proteintech Cat# 66744-1-Ig, RRID:AB\_2882092), LC3 I/II (Cell Signaling Technology Cat# 12741, RRID:AB\_2617131), Unc-51-like kinase (ULK1) (Proteintech Cat# 20986-1-AP, RRID:AB\_2878783), vascular endothelial (VE)-cadherin antibody (Abcam Cat# ab33168, RRID:AB\_870662), ZO-1 (Proteintech Cat# 21773-1-AP, RRID:AB\_10733242) and β-actin (Sigma-Aldrich Cat# A5441, RRID:AB\_476744). The antibody-reactive bands were visualized using an enhanced chemiluminescence Western blotting detection system (Millipore).

#### ***Statistical analysis***

The results are expressed as mean ± standard error of the mean (SEM). Statistical significance in experiments comparing only two groups was determined by a two-tailed Student's *t*-test. The comparison among multiple groups was estimated by one-way analysis of variance followed by *post-hoc* analysis using the Student-Newman-Keuls test. A P value of <0.05 was considered significant. All statistical analyses were done with SPSS 26.0 (SPSS Inc., Chicago, USA).

## **Results**

### ***Induction of autophagy in lung tissues of the endotoxemic mice and LPS-treated pulmonary VE cells***

We first examined the characteristic of autophagy in lung tissues of the endotoxemic mice. As shown in *Figure 1A*, pulmonary LC3-II expression was significantly elevated in the endotoxemic mice compared with the control mice. An ATG1 homologue in mammals, ULK1 is a key regulator in autophagy initiation (26). The present study found that LPS treatment significantly increased ULK1 expression in the lung tissues (*Figure 1A*).

As shown in *Figure 1B*, treatment of primary cultured MLVECs with increasing concentrations of LPS (10–1,000 ng/mL) caused significant increases in the protein levels of LC3-II and ULK1 in a dose-dependent manner over a 24-hour incubation period. Furthermore, we used a tandem fluorescence RFP-GFP-LC3 reporter system to monitor the autophagic flux in primary cultured MLVECs by confocal microscopy as previously reported (23). As shown in *Figure 1C,1D*, a marked increase in the number of both autophagosomes and autolysosomes was observed

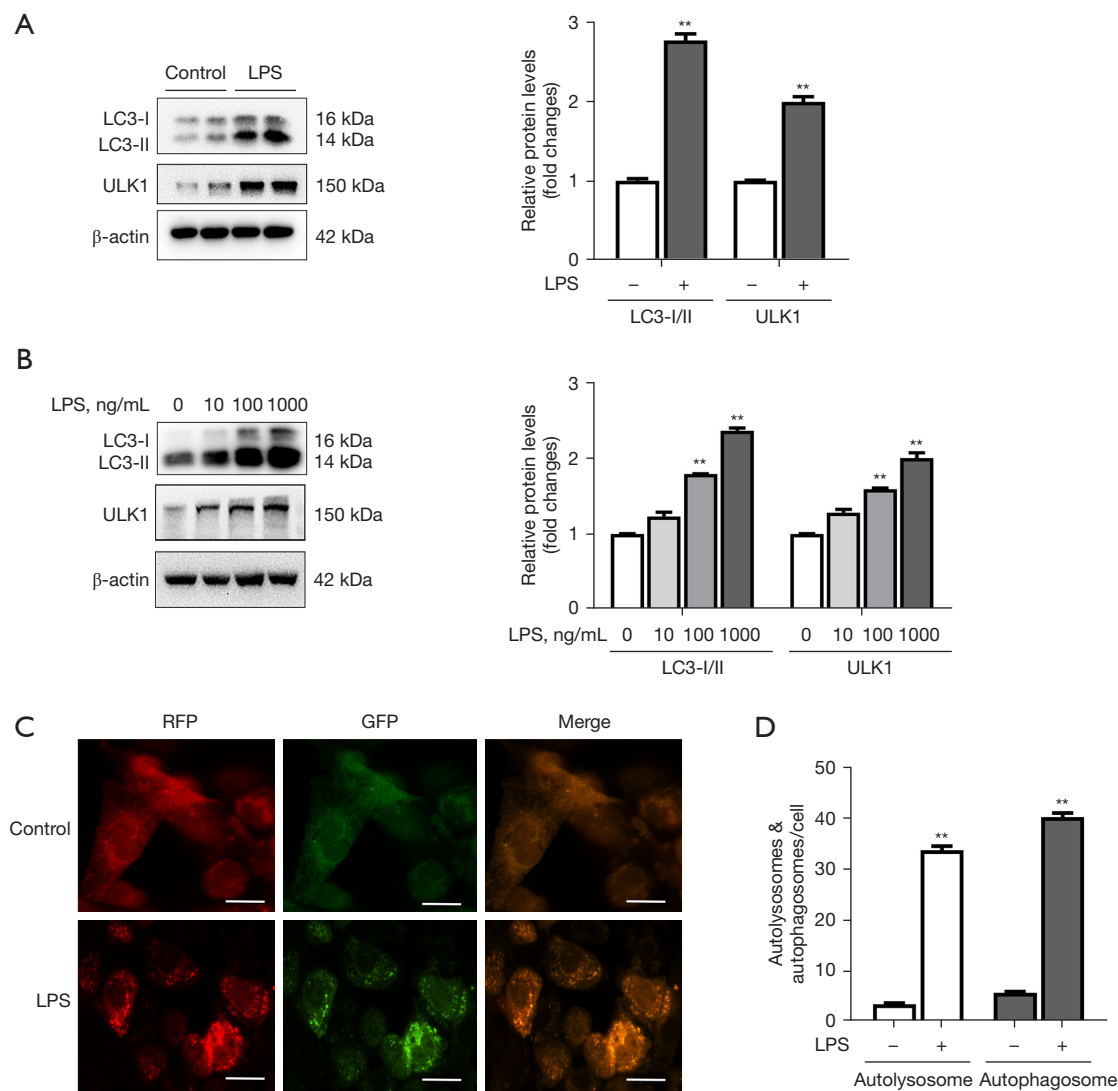


**Figure 1** Induction of autophagy in lung tissues of endotoxemic mice and LPS-treated pulmonary vascular endothelial cells. (A) Mice were intraperitoneally injected with LPS (30 mg/kg), the control group was injected with the same dose of saline. Twenty-four hours later, protein levels of LC3-I/II and ULK1 were determined by Western blot analysis. Corresponding histograms were shown on the right of protein bands (n=7). (B) MLVECs were treated with LPS at the indicated doses for 24 hours. Protein levels of LC3-I/II and ULK1 were determined by Western blot analysis. Corresponding histograms were shown on the right of protein bands (n=4). (C,D) MLVECs were transfected with RFP-GFP-LC3 adenoviral vector. Twenty-four hours later, cells were treated with LPS (1,000 ng/mL) for another 24 hours. (C) Representative images of RFP-GFP-LC3 puncta in MLVECs (n=4). Scale bars correspond to 50  $\mu$ m. (D) The number of autophagosomes and autolysosomes was shown in histograms (n=4). Data are presented as the mean  $\pm$  SEM. \*\*, P<0.01 vs. control group. LPS, lipopolysaccharide; MLVECs, mouse lung vascular endothelial cells; RFP-GFP-LC3, red fluorescent protein-green fluorescent protein tandem fluorescently-tagged LC3; SEM, standard error of the mean; ULK1, Unc-51-like kinase.

in MLVECs treated with LPS (1,000 ng/mL) for 24 hours. These observations indicated that autophagy had been induced in the lung tissues of endotoxemic mice and LPS-treated pulmonary VE cells.

### *Autophagy inhibition protects against LPS-induced pulmonary endothelial injury*

To investigate the contribution of autophagy in LPS-

induced pulmonary endothelial injury, the MLVECs were treated with autophagy inhibitor 3-methyladenine (3-MA) (10 mM) and exposed to 1,000 ng/mL LPS for 24 hours. It is well known that the VE-specific adherens junction molecule, VE-cadherin, and the tight-junction protein, ZO-1, play important roles in maintaining the integrity of the endothelial barrier (27). As shown in *Figure 2A*, the MLVECs exposed to LPS showed decreased protein levels of VE-cadherin and ZO-1, which were significantly reversed by pretreatment with 3-MA. Consistent with the Western blot results, immunofluorescence staining showed that 3-MA pretreatment significantly blocked the LPS-induced loss of ZO-1 in the plasma membrane of MLVECs (*Figure 2B,2C*). We then measured the permeability of a confluent endothelial monolayer for 10 kDa FITC-dextran. As shown in *Figure 2D*, 3-MA pretreatment significantly alleviated LPS-induced endothelial cell hyperpermeability.

We then investigated whether knockdown of the core autophagy gene, *ATG5*, affected LPS-induced pulmonary endothelial injury. As shown in *Figure 2E*, siRNA-mediated *ATG5* knockdown not only led to a significant decrease of *ATG5* expression in MLVECs, but also blocked the LPS-induced upregulation of *ATG5*. Knockdown of *ATG5* blocked the LPS-induced decreases in protein levels of VE-cadherin and ZO-1 (*Figure 2E*). Immunofluorescence staining showed that *ATG5* knockdown significantly reversed the LPS-induced loss of ZO-1 in MLVECs (*Figure 2F,2G*). Furthermore, LPS-induced endothelial cell hyperpermeability was also significantly alleviated by *ATG5* knockdown (*Figure 2H*). Collectively, these results indicated that autophagy inhibition could attenuate LPS-induced pulmonary endothelial injury.

#### ***FOXO1 is upregulated in lung tissues of endotoxemic mice and LPS-treated pulmonary VE cells***

The transcriptional factor FOXO1 is closely related to autophagy (28). As shown in *Figure 3A,3B*, pulmonary levels of both phosphorylated-FOXO1 and FOXO1 were significantly elevated in the endotoxemic mice compared with control mice. In addition, treatment of primary cultured MLVECs with increasing concentrations of LPS (10–1,000 ng/mL) caused significant increases in the protein levels of both phosphorylated-FOXO1 and FOXO1 in a dose-dependent manner over a 24-hour incubation period (*Figure 3C,3D*). Moreover, immunofluorescence staining showed that LPS treatment led to profound FOXO1 nuclear translocation in MLVECs (*Figure S1*).

#### ***Inhibition or knockdown of FOXO1 suppresses LPS-induced autophagy in pulmonary VE cells***

To investigate whether FOXO1 upregulation contributed to LPS-induced autophagy, primary cultured MLVECs were treated with the FOXO1 inhibitor AS1842856 (10  $\mu$ M) and exposed to 1,000 ng/mL LPS for 24 hours. AS1842856 is known to predominantly suppresses FOXO1-mediated transactivation by directly binding to FOXO1 (29). As shown in *Figure 4A* and *Figure S1*, AS1842856 pretreatment significantly decreased LPS-induced FOXO1 phosphorylation and FOXO1 nuclear translocation in MLVECs. The LPS-induced upregulation of autophagy-related proteins, LC3-II and ULK1, in the MLVECs was also blocked by AS1842856 pretreatment. Moreover, the number of both autophagosomes and autolysosomes in the LPS-treated MLVECs was significantly reduced by AS1842856 pretreatment (*Figure 4B,4C*).

We then investigated whether *FOXO1* knockdown affected LPS-induced autophagy in the MLVECs. As shown in *Figure 4D*, siRNA-mediated *FOXO1* knockdown not only led to a significant decrease in FOXO1 expression in the MLVECs, but also blocked the LPS-induced upregulation of FOXO1. Knockdown of *FOXO1* blocked the LPS-induced increases in protein levels of LC3-II and ULK1 (*Figure 4D*). As shown in *Figure 4E,4F*, *FOXO1* knockdown significantly reduced the number of both autophagosomes and autolysosomes in the LPS-treated MLVECs. Taken together, these findings indicated that FOXO1 inhibition or knockdown could suppress LPS-induced autophagy in pulmonary VE cells.

#### ***Inhibition or knockdown of FOXO1 protects against LPS-induced pulmonary endothelial injury***

As shown in *Figure 5A*, pretreatment with FOXO1 inhibitor AS1842856 (10  $\mu$ M) significantly alleviated LPS-induced downregulation of VE-cadherin and ZO-1. Consistent with the Western blot results, immunofluorescence staining showed that AS1842856 treatment significantly blocked the LPS-induced loss of ZO-1 in the plasma membrane of the MLVECs (*Figure 5B,5C*). Additionally, AS1842856 pretreatment significantly alleviated LPS-induced endothelial cell hyperpermeability, as evidenced by the profound reduction in FITC-dextran leakage (*Figure 5D*).

We then investigated whether *FOXO1* knockdown affected LPS-induced pulmonary endothelial injury. As shown in *Figure 5E*, *FOXO1* knockdown blocked the LPS-

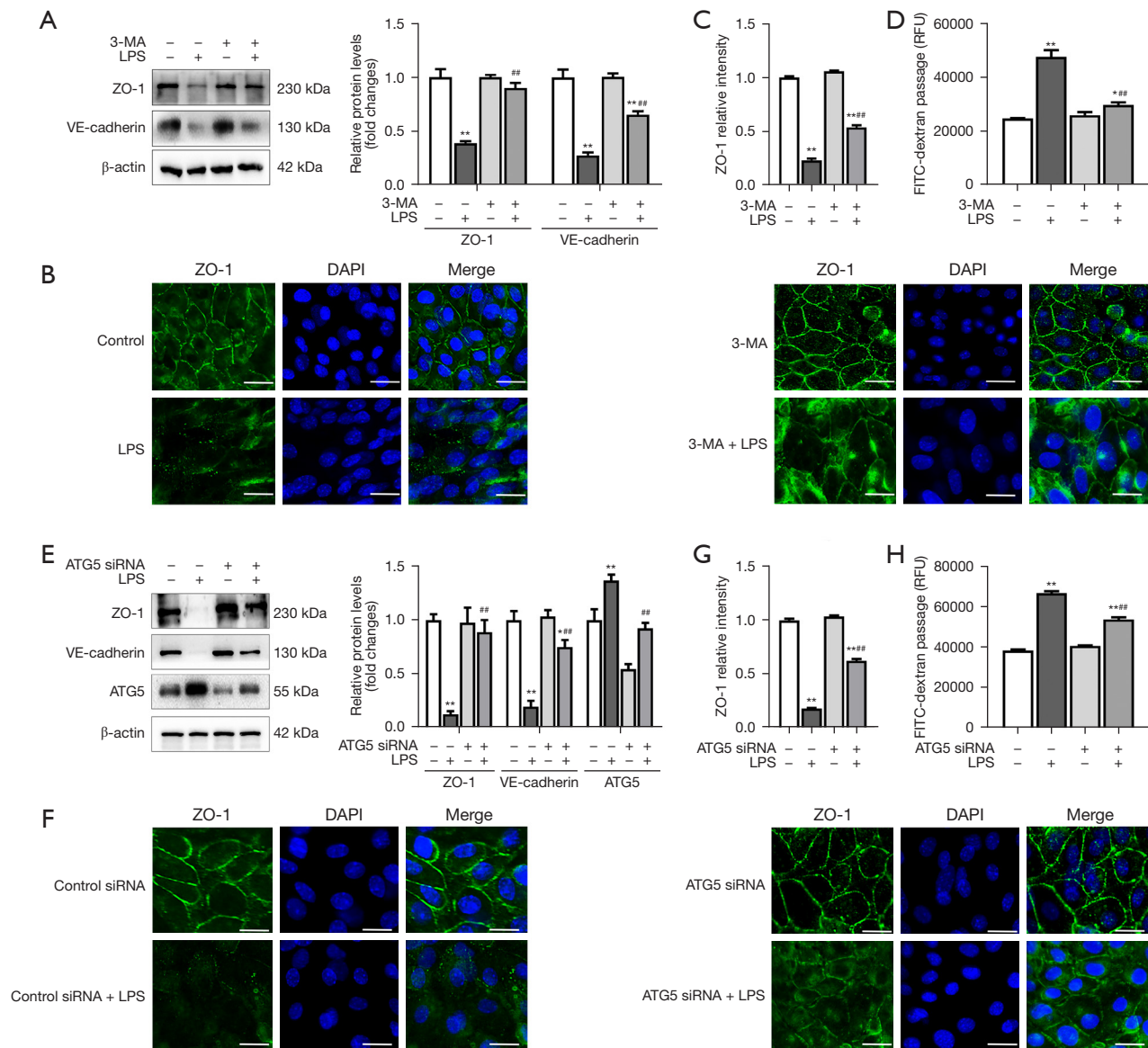


**Figure 2** Autophagy inhibition protects against LPS-induced pulmonary endothelial injury. (A-D) MLVECs were treated with LPS (1,000 ng/mL) with or without autophagy inhibitor 3-MA (10 mM) for 24 hours. (A) Representative protein bands of VE-cadherin and ZO-1. The corresponding histograms were presented on the right of the bands. (B) Representative immunofluorescent staining images showed that 3-MA reversed LPS-induced loss of ZO-1 (green) expression in MLVECs. Nuclei were counterstained with DAPI (blue). Original magnification,  $\times 200$ , scale bars correspond to 50  $\mu\text{m}$ . (C) The intensity of ZO-1 immunofluorescent staining was shown in histograms. (D) Endothelial permeability was determined by FITC-dextran flux assay. (E-H) MLVECs were transfected with control siRNA or siRNA targeting *ATG5*. Forty-eight hours later, cells were treated with or without LPS (1,000 ng/mL) for another 24 hours. (E) Representative protein bands of VE-cadherin, ZO-1 and *ATG5*. The corresponding histograms were presented on the right of the bands. (F) Representative immunofluorescent staining images showed that *ATG5* knockdown reversed LPS-induced loss of ZO-1 (green) expression in MLVECs. Nuclei were counterstained with DAPI (blue). Original magnification,  $\times 200$ , scale bars correspond to 50  $\mu\text{m}$ . (G) The intensity of ZO-1 immunofluorescent staining was shown in histograms. (H) Endothelial permeability was determined by FITC-dextran flux assay. Data are presented as the mean  $\pm$  SEM ( $n=4$ ). \*,  $P<0.05$ ; \*\*,  $P<0.01$  vs. control group; ###,  $P<0.01$  vs. LPS group. *ATG5*, autophagy-related gene 5; DAPI, 4',6-diamidino-2-phenylindole; FITC, fluorescein isothiocyanate-carboxymethyl; LPS, lipopolysaccharide; MLVECs, mouse lung vascular endothelial cells; 3-MA, 3-methyladenine; RFU, relative fluorescence units; SEM, standard error of the mean; VE, vascular endothelial; ZO-1, zonula occludens-1.

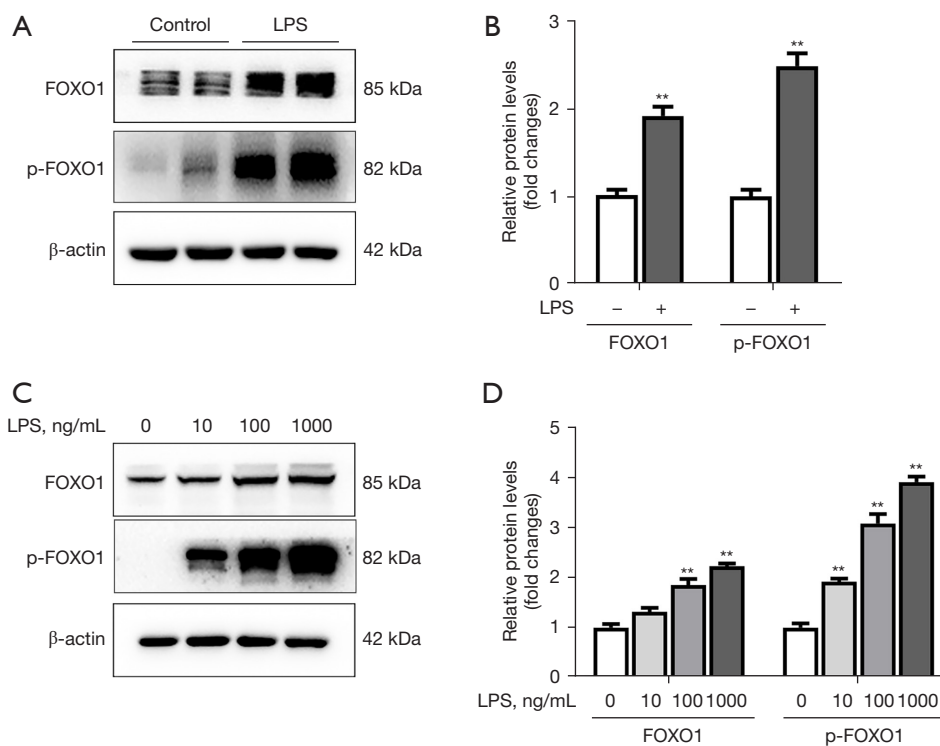


**Figure 3** Pulmonary level of FOXO1 is upregulated in endotoxemic mice and LPS-treated pulmonary vascular endothelial cells. (A) Mice were intraperitoneally injected with LPS (30 mg/kg), the control group was injected with the same dose of saline (n=7). Twenty-four hours later, protein levels of FOXO1 and phosphorylated-FOXO1 were determined by Western blot analysis. (B) Corresponding histograms were shown on the right of protein bands. (C) MLVECs were treated with LPS at the indicated doses for 24 hours (n=4). Protein levels of FOXO1 and phosphorylated-FOXO1 were determined by Western blot analysis. (D) Corresponding histograms were shown on the right of protein bands. Data are presented as the mean  $\pm$  SEM. \*\*,  $P < 0.01$  vs. control group. FOXO1, forkhead box O1; LPS, lipopolysaccharide; MLVECs, mouse lung vascular endothelial cells; SEM, standard error of the mean.

induced decreases in the protein levels of VE-cadherin and ZO-1. Immunofluorescence staining showed that *FOXO1* knockdown significantly reversed the LPS-induced loss of ZO-1 in the MLVECs (Figure 5F,5G). Furthermore, LPS-induced endothelial cell hyperpermeability was also significantly alleviated by *FOXO1* knockdown (Figure 5H). Collectively, these results indicated that FOXO1 inhibition or knockdown protected against LPS-induced pulmonary endothelial injury.

#### ***FOXO1* inhibition alleviates autophagy and acute injury in lung tissues of the endotoxemic mice**

We then examined the effect of the FOXO1 inhibitor AS1842856 on LPS-induced autophagy and ALI *in vivo*. As shown in Figure 6A, administration of AS1842856 significantly decreased LPS-induced upregulation of

phosphorylated-FOXO1 as well as the autophagy-related proteins, LC3-II and ULK1, in lung tissues of the endotoxemic mice. Protective effects of AS1842856 against endotoxemia-associated pulmonary VE injury were further assessed by measurements of VE-cadherin and ZO-1 expression as well as Evans blue dye leakage into the lung tissue. As shown in Figure 6B, LPS treatment led to decreased VE-cadherin and ZO-1 expression, as well as increased Evans blue dye leakage from the vascular space into the lung parenchyma, which was significantly reversed by AS1842856 treatment (Figure 6C).

Sections of lung tissue were stained with H&E and scored by histopathologic analysis. As shown in Figure 7A, histological analysis of lung sections revealed that endotoxemia-associated ALI was characterized by diffuse interstitial edema, leukocyte recruitment, alveolar thickening, and a marked decrease in the alveolar air

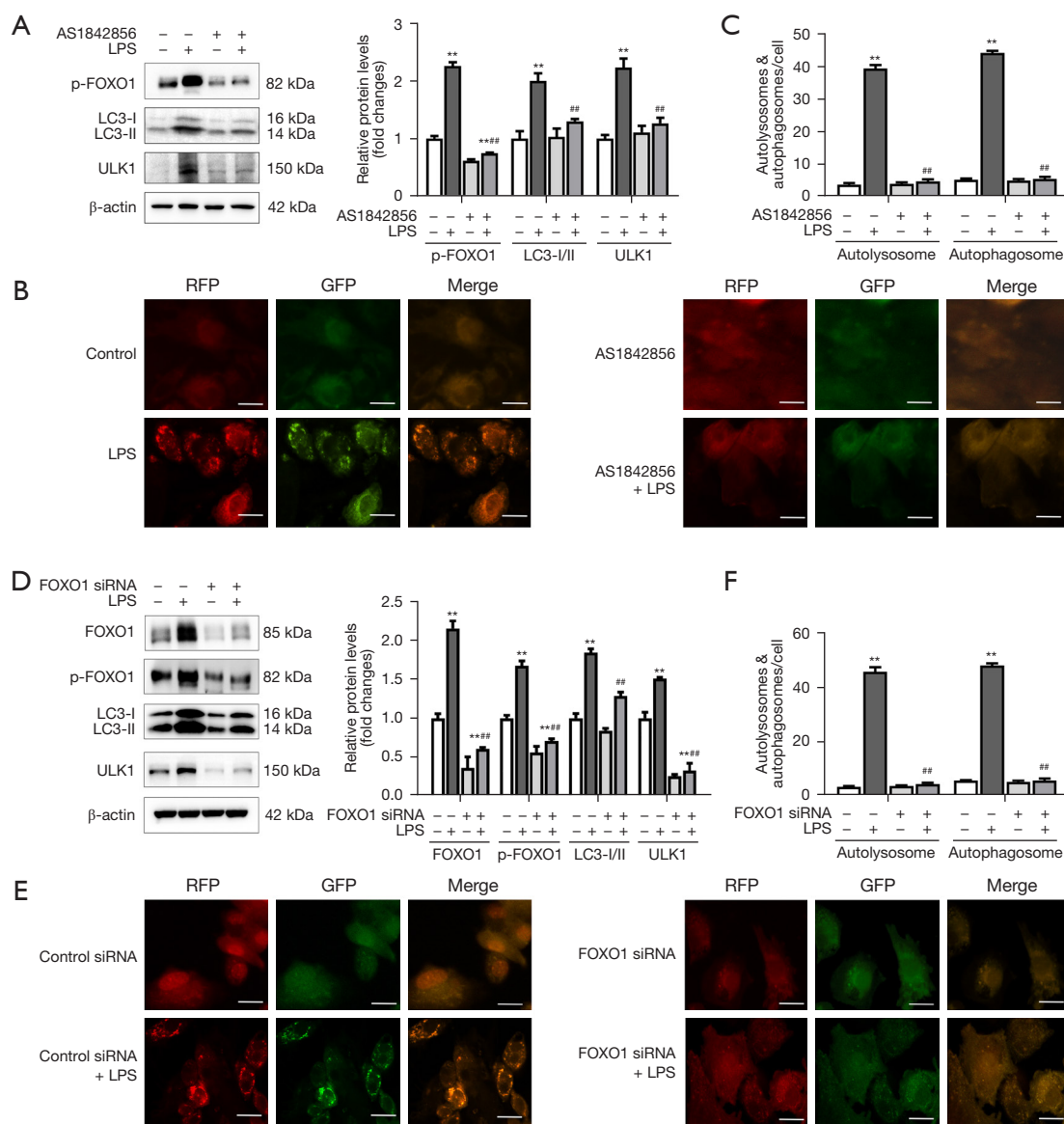


**Figure 4** Inhibition or knockdown of FOXO1 suppresses LPS-induced autophagy in pulmonary vascular endothelial cells. (A) MLVECs were treated with LPS (1,000 ng/mL) with or without FOXO1 inhibitor AS1842856 (10  $\mu$ M) for 24 hours. Protein levels of phosphorylated-FOXO1, LC3-I/II and ULK1 were determined by Western blot analysis. Corresponding histograms were shown on the right of protein bands. (B,C) MLVECs were transfected with RFP-GFP-LC3 adenoviral vector. Twenty-four hours later, cells were treated with LPS (1,000 ng/mL) with or without FOXO1 inhibitor AS1842856 (10  $\mu$ M) for another 24 hours. (B) Representative images of RFP-GFP-LC3 puncta in MLVECs (n=4). Scale bars correspond to 50  $\mu$ m. (C) The number of autophagosomes and autolysosomes was shown in histograms. (D) MLVECs were transfected with control siRNA or siRNA targeting *FOXO1*. Forty-eight hours later, cells were treated with or without LPS (1,000 ng/mL) for another 24 hours. Protein levels of FOXO1, phosphorylated-FOXO1, LC3-I/II and ULK1 were determined by Western blot analysis. The corresponding histograms were presented on the right of the bands. (E,F) MLVECs were transfected with RFP-GFP-LC3 adenoviral vector with control siRNA or siRNA targeting *FOXO1*. Forty-eight hours later, cells were treated with or without LPS (1,000 ng/mL) for another 24 hours. (E) Representative images of RFP-GFP-LC3 puncta in MLVECs (n=4). Scale bars correspond to 50  $\mu$ m. (F) The number of autophagosomes and autolysosomes was shown in histograms. Data are presented as the mean  $\pm$  SEM (n=4). \*\*, P<0.01 vs. control group; #, P<0.01 vs. LPS group. FOXO1, forkhead box O1; LPS, lipopolysaccharide; MLVECs, mouse lung vascular endothelial cells; RFP-GFP-LC3, red fluorescent protein-green fluorescent protein tandem fluorescent-tagged LC3; SEM, standard error of the mean; ULK1, Unc-51-like kinase.

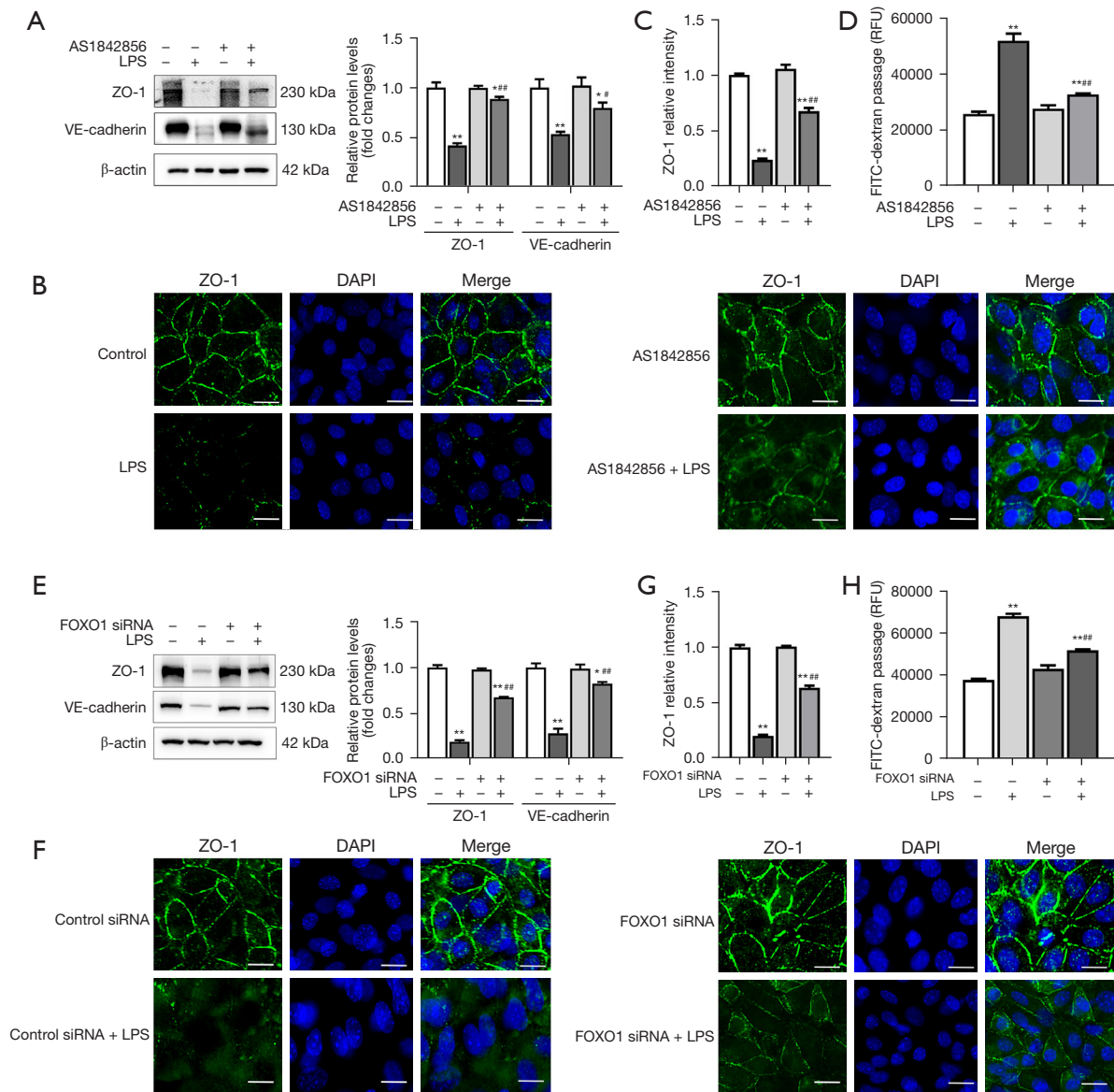


**Figure 5** Inhibition or knockdown of FOXO1 protects against LPS-induced pulmonary endothelial injury. (A-D) MLVECs were treated with LPS (1,000 ng/mL) with or without FOXO1 inhibitor AS1842856 (10  $\mu$ M) for 24 hours. (A) Representative protein bands of VE-cadherin and ZO-1. The corresponding histograms were presented on the right of the band. (B) Representative immunofluorescent staining images showed that AS1842856 reversed LPS-induced loss of ZO-1 (green) expression in MLVECs. Nuclei were counterstained with DAPI (blue). Original magnification,  $\times 200$ , scale bars correspond to 50  $\mu$ m. (C) The intensity of ZO-1 immunofluorescent staining was shown in histograms. (D) Endothelial permeability was determined by FITC-dextran flux assay. (E-H) MLVECs were transfected with control siRNA or siRNA targeting *FOXO1*. Forty-eight hours later, cells were treated with or without LPS (1,000 ng/mL) for another 24 hours. (E) Representative protein bands of VE-cadherin and ZO-1. The corresponding histograms were presented on the right of the bands. (F) Representative immunofluorescent staining images showed that *FOXO1* knockdown reversed LPS-induced loss of ZO-1 (green) expression in MLVECs. Nuclei were counterstained with DAPI (blue). Original magnification,  $\times 200$ , scale bars correspond to 50  $\mu$ m. (G) The intensity of ZO-1 immunofluorescent staining was shown in histograms. (H) Endothelial permeability was determined by FITC-dextran flux assay. Data are presented as the mean  $\pm$  SEM (n=4). \*, P<0.05; \*\*, P<0.01 vs. control group; #, P<0.05; ###, P<0.01 vs. LPS group. DAPI, 4',6-diamidino-2-phenylindole; FITC, fluorescein isothiocyanate-carboxymethyl; FOXO1, forkhead box O1; LPS, lipopolysaccharide; MLVECs, mouse lung vascular endothelial cells; RFU, relative fluorescence units; SEM, standard error of the mean; VE, vascular endothelial; ZO-1, zonula occludens-1.

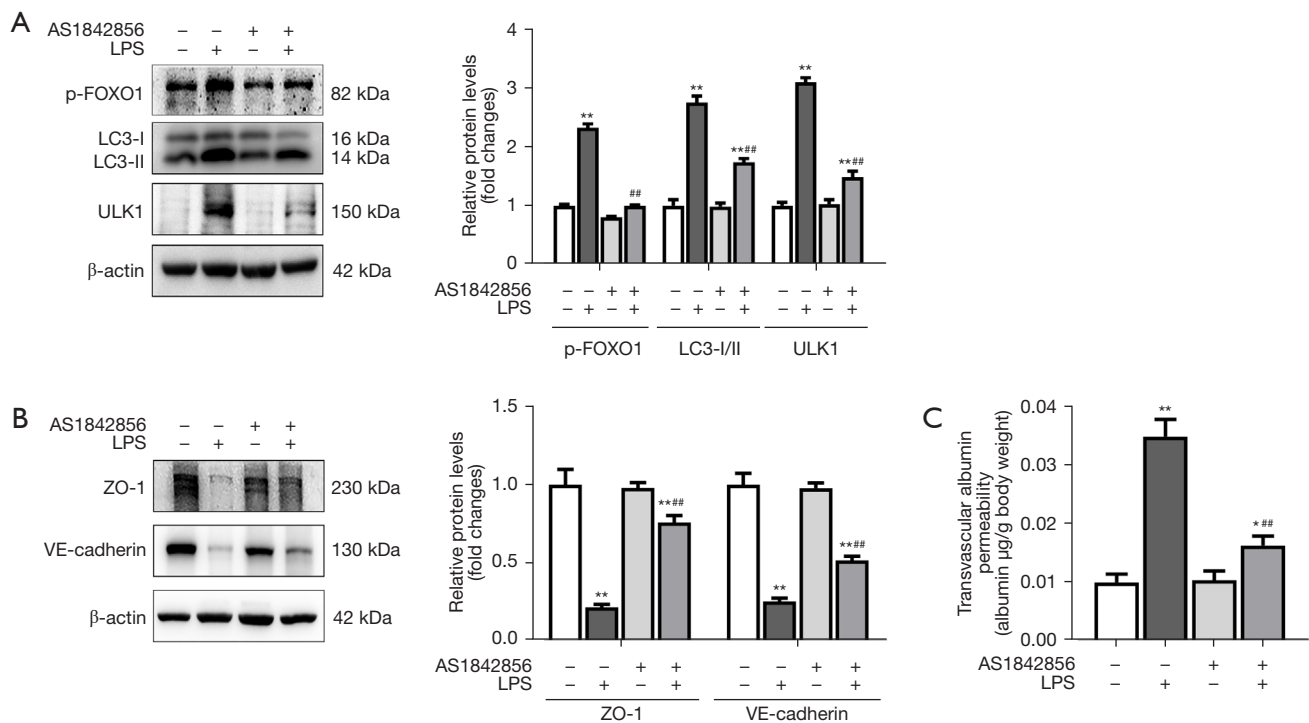


**Figure 6** FOXO1 inhibition alleviates autophagy and acute injury in lung tissues of endotoxemic mice. Mice were intraperitoneally injected with LPS (30 mg/kg). FOXO1 inhibitor AS1842856 (30 mg/kg) was intragastrically injected 30 minutes before the injection of LPS, with an equivalent volume of saline intragastrically injected in other groups. Twenty-four hours later, protein levels of phosphorylated-FOXO1, LC3-I/II and ULK1 (A), VE-cadherin and ZO-1 (B) were determined by Western blot analysis. Corresponding histograms were shown on the right of protein bands. Pulmonary vascular permeability was quantified by Evans Blue dye extravasation assay (C). Data are presented as the mean  $\pm$  SEM (n=7). \*, P<0.05; \*\*, P<0.01 vs. control group; ##, P<0.01 vs. LPS group. FOXO1, forkhead box O1; LPS, lipopolysaccharide; SEM, standard error of the mean; VE, vascular endothelial; ULK1, Unc-51-like kinase; ZO-1, zonula occludens-1.

space, with a histopathologic damage score of  $3.87 \pm 0.084$  (Figure 7B). These effects were significantly alleviated by AS1842856 treatment, and the lung injury score was reduced to  $1.93 \pm 0.12$  (Figure 7B).

## Discussion

Autophagy has been reported to be activated during the pathogenesis of endothelial dysfunction and ALI (10,13); however, whether autophagy induced during endothelial injury is beneficial or detrimental remains controversial. For example, LPS induces autophagy in human pulmonary microvascular endothelial cells (HPMVECs) (30). Inhibiting autophagy by blocking ATG7 or ATG5 expression, or by the autophagy inhibitor, chloroquine, aggravates LPS-induced high permeability of HPMVECs (30). Inhibition of ATG7 expression has also been found to markedly weaken the protective effects of adipose-derived stem cells on LPS-

induced microvascular barrier injury (31). In contrast, Slavin *et al.* found that administration of the autophagy inhibitor, 3-MA, either prophylactically or therapeutically, markedly reduced LPS-induced lung vascular leakage and tissue edema (10). In cultured human aortic endothelial cells, Zhang *et al.* reported that 3-MA, but not chloroquine, blunted the advanced glycation end-product-induced apoptosis (32). The discrepancy might be due to the different agents and approaches used to block autophagy. Consistent with the findings of Slavin *et al.* and Zhang *et al.*, the present study provided evidence that inhibiting autophagy by 3-MA or knockdown of *ATG5* significantly alleviated LPS-induced lung endothelial hyperpermeability, suggesting that inhibition of autophagy protected against endothelial cell barrier dysfunction.

Endothelial autophagy is controlled by several signaling pathways. In response to metabolic stresses such as amino acid starvation and growth factor deprivation, the mechanistic

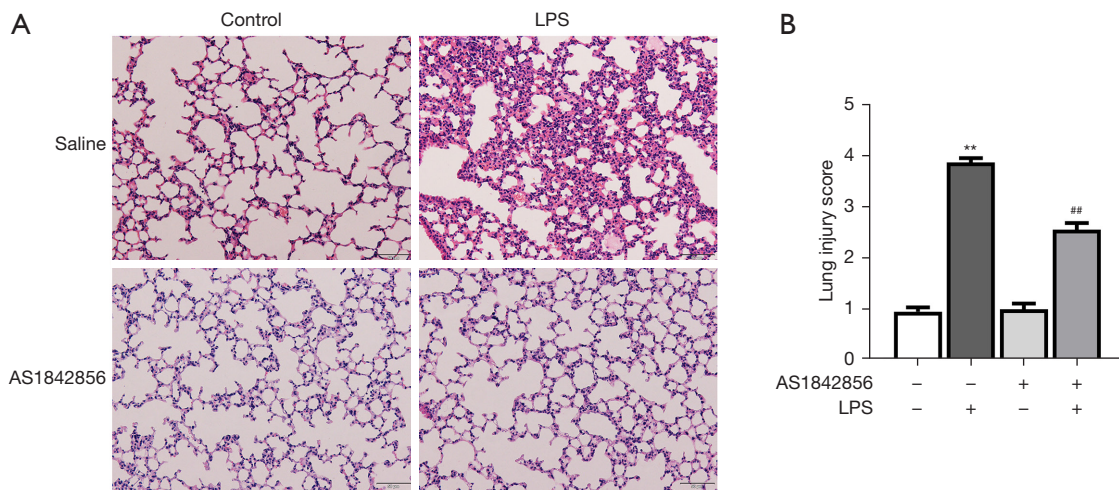


**Figure 7** FOXO1 inhibition attenuates LPS-induced acute lung injury. (A) Mice were intraperitoneally injected with LPS (30 mg/kg). FOXO1 inhibitor AS1842856 (30 mg/kg) was intragastrically injected 30 minutes before the injection of LPS, with an equivalent volume of saline intragastrically injected in other groups. Twenty-four hours later, lung tissues were used for histological evaluation by H&E staining. (B) The severity of lung injury was scored by two pathologists blinded to group allocation. Original magnification,  $\times 200$ . Scale bars correspond to 50  $\mu\text{m}$ . Data are presented as the mean  $\pm$  SEM ( $n=7$ ). \*\*,  $P<0.01$  vs. control group; ##,  $P<0.01$  vs. LPS group. FOXO1, forkhead box O1; H&E, hematoxylin and eosin; LPS, lipopolysaccharide; SEM, standard error of the mean.

target of rapamycin complex 1 (mTORC1)-ULK1 pathway is a master regulator responsible for endothelial autophagy induction (33). Also, AMP-activated protein kinase (AMPK) can directly phosphorylate ULK1 and beclin-1, thereby activate the autophagy machinery in endothelial cells (33). In addition, accumulating evidence suggests that FOXO1 is involved in mediating endothelial autophagy induced by shear stress (34), oxidized low-density lipoprotein (ox-LDL) (35,36), and hydrogen sulfide (37). The present study demonstrated that LPS-induced autophagy was associated with an increased expression of FOXO1. Moreover, treatment with the FOXO1 inhibitor AS1842856 or *FOXO1* siRNA profoundly suppressed autophagy in LPS-treated pulmonary VE cells. AS1842856 also alleviated autophagy in lung tissues of the endotoxemic mice. These findings indicate that FOXO1 upregulation is an important contributor to endothelial autophagy induced by LPS.

It has been recognized that FOXO1 is a crucial regulator of cell metabolism in several tissues, including the endothelium, controlling the levels of some relevant biomarkers in atherosclerotic processes (38). In fact, the over-expression of FOXO1 in human umbilical endothelial cells is associated with decreased nitric oxide (NO) bioavailability, increased oxidative stress, and inflammation (39). Endothelial cell-directed deletion of *FOXO1* in adult mice induces

excessive endothelial proliferation coupled with reduced apoptosis (38). These findings indicate that FOXO1 is a suppressor of endothelial growth and proliferation and imply the pro-apoptotic effect of FOXO1 in endothelial cells. To date, whether and how FOXO1 contributes to the development of endothelial dysfunction in ALI remains largely unknown. Artham *et al.* recently demonstrated that pharmacological inhibition or lentivirus-mediated knockdown of *FOXO1/3a* has beneficial effects on LPS-induced lung injury and edema (16). The present study provided several lines of evidence that the pharmacological inhibition of FOXO1 or siRNA-mediated *FOXO1* knockdown significantly alleviated pulmonary endothelial dysfunction associated with endotoxemia. Treatment with FOXO1 inhibitor or *FOXO1* siRNA alleviated LPS-induced downregulation of VE-cadherin and ZO-1 and resulted in profound reduction in FITC-dextran leakage *in vitro*. The protective effects of FOXO1 inhibitor against pulmonary VE injury were also confirmed in the endotoxemic mice. Notably, this study also recognized FOXO1 as an important contributor to LPS-induced endothelial autophagy, which contributes to LPS-induced endothelial hyperpermeability. Collectively, these data suggest that the detrimental effects of FOXO1 in endotoxemia-associated endothelial dysfunction and ALI may be partly due to its potent pro-autophagy

property.

Previous studies have shown that LPS can increase the expression of FOXO1 in skeletal muscles (40,41), macrophages (42), and nucleus pulposus cells (43). Consistent with our results, Sun *et al.* found an upregulation of pulmonary FOXO1 expression in a rat model of LPS-induced lung injury (44). However, the exact mechanism underlying the effect of LPS on regulating FOXO1 expression remains unknown. Notably, the gene expression of *FOXO1* is regulated by 2 transcription factors, E2F transcription factor 1 (E2F-1) and the chromatin factor high-mobility group A1 (HMGA1) (45,46), both of which are known to contribute to LPS-induced inflammatory responses (47,48). These findings let us suggest that LPS might increase FOXO1 expression via E2F-1 and/or HMGA1-dependent pathways, which merits future investigation.

Certain limitations should be considered regarding this study. First, FOXO1 has the additional non-autophagy related cellular effects on endothelial cell injury and is also involved in endothelial cell apoptosis (32,49). The benefits of FOXO1 inhibition illustrated in this study might not be entirely attributed to its inhibitive effect on autophagy. Second, this study used LPS-induced ALI model alone to investigate the contribution of FOXO1 to endothelial cell autophagy and dysfunction. Confirmation of the role of FOXO1 in other animal models such as ALI-induced by cecal ligation and puncture, acid aspiration, or mechanical ventilation would further reinforce the choice of FOXO1 as a potential therapeutic target.

In summary, the present study demonstrated for the first time that FOXO1 upregulation is an important contributor to LPS-induced autophagy in pulmonary VE cells and lung tissues of endotoxemic mice. In addition, this study provided both *in vivo* and *in vitro* evidence that FOXO1 inhibitor profoundly suppressed LPS-induced endothelial autophagy and damage, suggesting that the detrimental effects of FOXO1 in endotoxemia-associated endothelial dysfunction and ALI may be partly due to its potent pro-autophagy property. The data obtained in this study provide supportive evidence for the theory that inhibition of FOXO1 may be a potential therapeutic option for the treatment of ALI.

## Acknowledgments

**Funding:** This work was supported by the National Natural Science Foundation of China (Nos. 31871156, 32171124, 81672266, 82072209) and the Shanghai Frontiers Science

Research Base of Exercise and Metabolic Health.

## Footnote

**Reporting Checklist:** The authors have completed the ARRIVE reporting checklist. Available at <https://atm.amegroups.com/article/view/10.21037/atm-21-5380/rc>

**Data Sharing Statement:** Available at <https://atm.amegroups.com/article/view/10.21037/atm-21-5380/dss>

**Peer Review File:** Available at <https://atm.amegroups.com/article/view/10.21037/atm-21-5380/prf>

**Conflicts of Interest:** All authors have completed the ICMJE uniform disclosure form (available at <https://atm.amegroups.com/article/view/10.21037/atm-21-5380/coif>). All authors report funding from the National Natural Science Foundation of China (Nos. 31871156, 32171124, 81672266, 82072209) and the Shanghai Frontiers Science Research Base of Exercise and Metabolic Health. The authors have no other conflicts of interest to declare.

**Ethical Statement:** The authors are accountable for all aspects of the work to ensure that issues related to the accuracy or integrity of any part of the work are properly investigated and resolved. Experiments were performed under a project license (No. 2016014) granted by the Animal Ethics Committee of Shanghai Sports University and in accordance with the National Institutes of Health guidelines for the care and use of animals.

**Open Access Statement:** This is an Open Access article distributed in accordance with the Creative Commons Attribution-NonCommercial-NoDerivs 4.0 International License (CC BY-NC-ND 4.0), which permits the non-commercial replication and distribution of the article with the strict proviso that no changes or edits are made and the original work is properly cited (including links to both the formal publication through the relevant DOI and the license). See: <https://creativecommons.org/licenses/by-nc-nd/4.0/>.

## References

- Jarczak D, Kluge S, Nierhaus A. Sepsis-Pathophysiology and Therapeutic Concepts. *Front Med (Lausanne)* 2021;8:628302.
- Rudd KE, Johnson SC, Agesa KM, et al. Global, regional,

- and national sepsis incidence and mortality, 1990-2017: analysis for the Global Burden of Disease Study. *Lancet* 2020;395:200-11.
3. Kumar V. Pulmonary Innate Immune Response Determines the Outcome of Inflammation During Pneumonia and Sepsis-Associated Acute Lung Injury. *Front Immunol* 2020;11:1722.
  4. Matthay MA, Zemans RL, Zimmerman GA, et al. Acute respiratory distress syndrome. *Nat Rev Dis Primers* 2019;5:18.
  5. Liu M, Zhang L, Marsboom G, et al. Sox17 is required for endothelial regeneration following inflammation-induced vascular injury. *Nat Commun* 2019;10:2126.
  6. Xiong S, Hong Z, Huang LS, et al. IL-1 $\beta$  suppression of VE-cadherin transcription underlies sepsis-induced inflammatory lung injury. *J Clin Invest* 2020;130:3684-98.
  7. Zhou Y, Li P, Goodwin AJ, et al. Exosomes from endothelial progenitor cells improve outcomes of the lipopolysaccharide-induced acute lung injury. *Crit Care* 2019;23:44.
  8. Schmidt EP, Yang Y, Janssen WJ, et al. The pulmonary endothelial glycocalyx regulates neutrophil adhesion and lung injury during experimental sepsis. *Nat Med* 2012;18:1217-23.
  9. Mizushima N, Levine B. Autophagy in Human Diseases. *N Engl J Med* 2020;383:1564-76.
  10. Slavin SA, Leonard A, Grose V, et al. Autophagy inhibitor 3-methyladenine protects against endothelial cell barrier dysfunction in acute lung injury. *Am J Physiol Lung Cell Mol Physiol* 2018;314:L388-96.
  11. Lu LH, Chao CH, Yeh TM. Inhibition of autophagy protects against sepsis by concurrently attenuating the cytokine storm and vascular leakage. *J Infect* 2019;78:178-86.
  12. Zhang RH, Zhang HL, Li PY, et al. Autophagy is involved in the acute lung injury induced by H9N2 influenza virus. *Int Immunopharmacol* 2019;74:105737.
  13. Zhao H, Chen H, Xiaoyin M, et al. Autophagy Activation Improves Lung Injury and Inflammation in Sepsis. *Inflammation* 2019;42:426-39.
  14. Xing YQ, Li A, Yang Y, et al. The regulation of FOXO1 and its role in disease progression. *Life Sci* 2018;193:124-31.
  15. Andrade J, Shi C, Costa ASH, et al. Control of endothelial quiescence by FOXO-regulated metabolites. *Nat Cell Biol* 2021;23:413-23.
  16. Artham S, Gao F, Verma A, et al. Endothelial stromelysin1 regulation by the forkhead box-O transcription factors is crucial in the exudative phase of acute lung injury. *Pharmacol Res* 2019;141:249-63.
  17. Jiang R, Xu J, Zhang Y, et al. Ligustrazine Alleviate Acute Lung Injury Through Suppressing Pyroptosis and Apoptosis of Alveolar Macrophages. *Front Pharmacol* 2021;12:680512.
  18. Dong WW, Liu YJ, Lv Z, et al. Lung endothelial barrier protection by resveratrol involves inhibition of HMGB1 release and HMGB1-induced mitochondrial oxidative damage via an Nrf2-dependent mechanism. *Free Radic Biol Med* 2015;88:404-16.
  19. Xu CF, Liu YJ, Wang Y, et al. Downregulation of R-Spondin1 Contributes to Mechanical Stretch-Induced Lung Injury. *Crit Care Med* 2019;47:e587-96.
  20. Zheng W, Qian Y, Chen S, et al. Rapamycin Protects Against Peritendinous Fibrosis Through Activation of Autophagy. *Front Pharmacol* 2018;9:402.
  21. Shen Y, Xu W, You H, et al. FoxO1 inhibits transcription and membrane trafficking of epithelial Na<sup>+</sup> channel. *J Cell Sci* 2015;128:3621-30.
  22. Chakrabarti P, Kandror KV. FoxO1 controls insulin-dependent adipose triglyceride lipase (ATGL) expression and lipolysis in adipocytes. *J Biol Chem* 2009;284:13296-300.
  23. Xiao C, Wang K, Xu Y, et al. Transplanted Mesenchymal Stem Cells Reduce Autophagic Flux in Infarcted Hearts via the Exosomal Transfer of miR-125b. *Circ Res* 2018;123:564-78.
  24. Zhang H, Mao YF, Zhao Y, et al. Upregulation of Matrix Metalloproteinase-9 Protects against Sepsis-Induced Acute Lung Injury via Promoting the Release of Soluble Receptor for Advanced Glycation End Products. *Oxid Med Cell Longev* 2021;2021:8889313.
  25. Wang Y, Liu YJ, Xu DF, et al. DRD1 downregulation contributes to mechanical stretch-induced lung endothelial barrier dysfunction. *Theranostics* 2021;11:2505-21.
  26. Hurley JH, Young LN. Mechanisms of Autophagy Initiation. *Annu Rev Biochem* 2017;86:225-44.
  27. Tornavaca O, Chia M, Dufton N, et al. ZO-1 controls endothelial adherens junctions, cell-cell tension, angiogenesis, and barrier formation. *J Cell Biol* 2015;208:821-38.
  28. Cheng Z. The FoxO-Autophagy Axis in Health and Disease. *Trends Endocrinol Metab* 2019;30:658-71.
  29. Nagashima T, Shigematsu N, Maruki R, et al. Discovery of novel forkhead box O1 inhibitors for treating type 2 diabetes: improvement of fasting glycemia in diabetic db/db mice. *Mol Pharmacol* 2010;78:961-70.
  30. Zhang D, Zhou J, Ye LC, et al. Autophagy maintains the

- integrity of endothelial barrier in LPS-induced lung injury. *J Cell Physiol* 2018;233:688-98.
31. Li C, Pan J, Ye L, et al. Autophagy regulates the therapeutic potential of adipose-derived stem cells in LPS-induced pulmonary microvascular barrier damage. *Cell Death Dis* 2019;10:804.
  32. Zhang H, Ge S, He K, et al. FoxO1 inhibits autophagosome-lysosome fusion leading to endothelial autophagic-apoptosis in diabetes. *Cardiovasc Res* 2019;115:2008-20.
  33. Li Y, Suo L, Fu Z, et al. Pivotal role of endothelial cell autophagy in sepsis. *Life Sci* 2021;276:119413.
  34. Liu J, Bi X, Chen T, et al. Shear stress regulates endothelial cell autophagy via redox regulation and Sirt1 expression. *Cell Death Dis* 2015;6:e1827.
  35. Zhu Z, Li J, Zhang X. Salidroside protects against ox-LDL-induced endothelial injury by enhancing autophagy mediated by SIRT1-FoxO1 pathway. *BMC Complement Altern Med* 2019;19:111.
  36. Yu F, Zhang Y, Wang Z, et al. Hsa\_circ\_0030042 regulates abnormal autophagy and protects atherosclerotic plaque stability by targeting eIF4A3. *Theranostics* 2021;11:5404-17.
  37. Zhu L, Duan W, Wu G, et al. Protective effect of hydrogen sulfide on endothelial cells through Sirt1-FoxO1-mediated autophagy. *Ann Transl Med* 2020;8:1586.
  38. Menghini R, Casagrande V, Iuliani G, et al. Metabolic aspects of cardiovascular diseases: Is FoxO1 a player or a target? *Int J Biochem Cell Biol* 2020;118:105659.
  39. Menghini R, Casagrande V, Cardellini M, et al. FoxO1 regulates asymmetric dimethylarginine via downregulation of dimethylaminohydrolase 1 in human endothelial cells and subjects with atherosclerosis. *Atherosclerosis* 2015;242:230-5.
  40. Valentine RJ, Jefferson MA, Kohut ML, et al. Imoxin attenuates LPS-induced inflammation and MuRF1 expression in mouse skeletal muscle. *Physiol Rep* 2018;6:e13941.
  41. Martín AI, Gómez-SanMiguel AB, Gómez-Moreira C, et al.  $\alpha$ MSH blunts endotoxin-induced MuRF1 and atrogen-1 upregulation in skeletal muscle by modulating NF- $\kappa$ B and Akt/FoxO1 pathway. *Mediators Inflamm* 2014;2014:179368.
  42. Wang LC, Wei WH, Zhang XW, et al. An Integrated Proteomics and Bioinformatics Approach Reveals the Anti-inflammatory Mechanism of Carnosic Acid. *Front Pharmacol* 2018;9:370.
  43. Chai X, Si H, Song J, et al. miR-486-5p Inhibits Inflammatory Response, Matrix Degradation and Apoptosis of Nucleus Pulposus Cells through Directly Targeting FOXO1 in Intervertebral Disc Degeneration. *Cell Physiol Biochem* 2019;52:109-18.
  44. Sun K, Huang R, Yan L, et al. Schisandrin Attenuates Lipopolysaccharide-Induced Lung Injury by Regulating TLR-4 and Akt/FoxO1 Signaling Pathways. *Front Physiol* 2018;9:1104.
  45. Arcidiacono B, Chiefari E, Messineo S, et al. HMGA1 is a novel transcriptional regulator of the FoxO1 gene. *Endocrine* 2018;60:56-64.
  46. Nowak K, Killmer K, Gessner C, et al. E2F-1 regulates expression of FOXO1 and FOXO3a. *Biochim Biophys Acta* 2007;1769:244-52.
  47. Lu W, Ji R. Identification of significant alteration genes, pathways and TFs induced by LPS in ARDS via bioinformatical analysis. *BMC Infect Dis* 2021;21:852.
  48. Cai ZL, Shen B, Yuan Y, et al. The effect of HMGA1 in LPS-induced Myocardial Inflammation. *Int J Biol Sci* 2020;16:1798-810.
  49. Xie Y, Li X, Ge J. Cyclophilin A-FoxO1 signaling pathway in endothelial cell apoptosis. *Cell Signal* 2019;61:57-65.

**Cite this article as:** Zhao Y, Zhang H, Zhang SL, Wei J, Zheng LL, Du JK, Zhu XY, Jiang L, Liu YJ. Upregulation of *FOXO1* contributes to lipopolysaccharide-induced pulmonary endothelial injury by induction of autophagy. *Ann Transl Med* 2022;10(11):630. doi: 10.21037/atm-21-5380

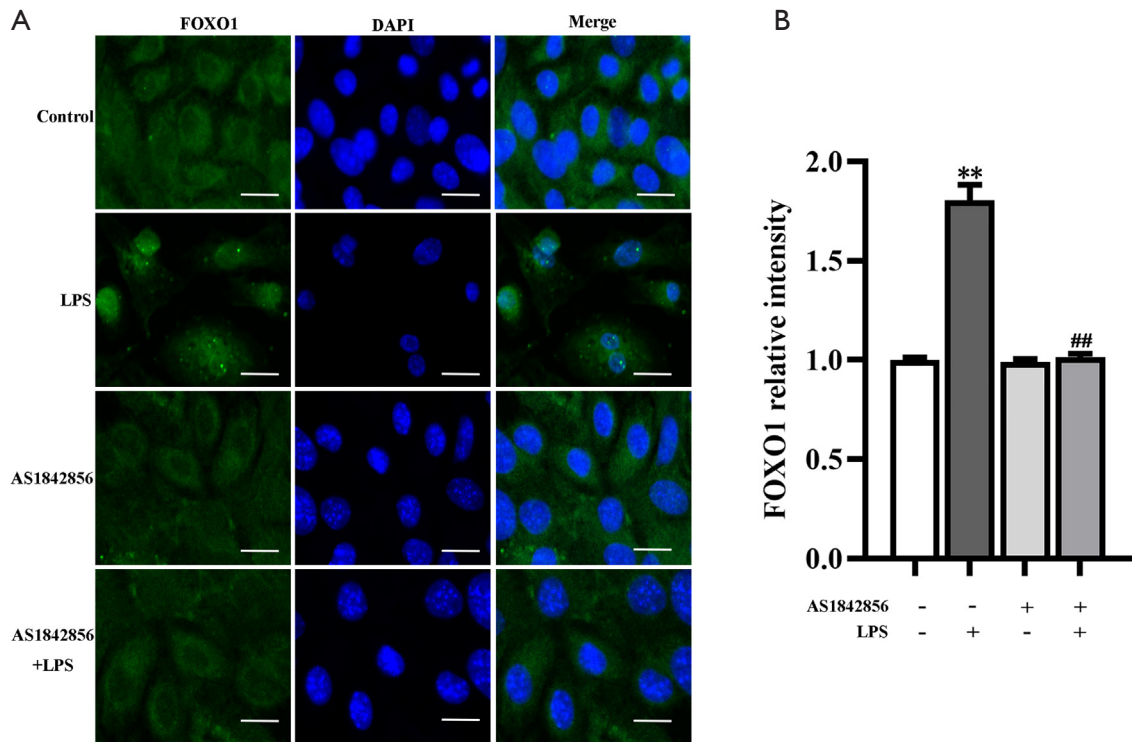


**Figure S1** FOXO1 inhibition reversed LPS-induced FOXO1 nuclear translocation. MLVECs were treated with LPS (1,000 ng/mL) with or without FOXO1 inhibitor AS1842856 (10  $\mu$ M) for 24 hours. (A) Immunofluorescent staining showed AS1842856 reversed LPS-induced nuclear translocation of FOXO1 (green). Nuclei were counterstained with DAPI (blue). Original magnification,  $\times 200$ , scale bars correspond to 50  $\mu$ m. (B) The intensity of FOXO1 immunofluorescent staining was shown in histograms. Data are presented as the mean  $\pm$  SEM (n=4). \*\*, P<0.01 vs. control group; ##, P<0.01 vs. LPS group. DAPI, 4',6-diamidino-2-phenylindole; FOXO1, forkhead Box O1; LPS, lipopolysaccharide; MLVECs, mouse lung vascular endothelial cells; SEM, standard error of the mean.